Journal of Applied Fluid Mechanics, Vol. 9, No. 1, pp. 407-418, 2016.
Available online at www.jafmonline.net, ISSN 1735-3572, EISSN 1735-3645.
DOI: 10.18869/acadpub.jafm.68.224.24187

Radial and Axial Magnetic Fields Effects on Natural Convection in a Nanofluid-filled Vertical Cylinder

M. Battira[1†] and R. Bessaih[2]

[1]*Department of Physics,Moulay Tahar University, Saida, 20000, Algeria*
[2]*Department of Mechanical Engineering, LEAP Laboratory, Constantine, 250000, Algeria*

†*Corresponding Author Email:mounamaache@yahoo.fr*

(Received November 6, 2014; accepted February 11, 2015)

ABSTRACT

This work aims to study numerically the steady natural convection in a vertical cylinder filled with an Al_2O_3 nanofluid under two different external magnetic fields (B_r, B_z) either in the radial or axial directions. The cylinder having an aspect ratio $H/R_0=1$ is bounded by the top and the bottom disks at temperatures T_c and T_h, and by an adiabatic side wall. The equations of continuity, Navier-Stokes and energy are non-dimensionalized and then discretized by the finite volume method. A computer program based on the SIMPLER algorithm is developed and compared with the numerical results found in the literature. The effects of nano-size solid volume fraction ranging from 0 to 0.1 and application of the magnetic field in either directions axial and radial for various values of Hartmann numbers on flow and thermal fields, and on local and average Nusselt numbers are presented and discussed for two values of Rayleigh numbers ($Ra=10^3$ and 10^4). The behaviors of average Nusselt number, streamlines, temperature contours, and the both components of velocity are illustrated. The results indicate that for small values of the Hartmann number, where the flow remains due to the convection, the average Nusselt number decreases when increasing the solid volume fraction and this decrease is more important if the magnetic field is applied in the axial direction and by increasing the Hartmann numbers. The increasing in the solid volume fraction increases the performance of heat transfer in the nanofluid.

Keywords: Natural convection; Nanofluid; Magnetic field.

NOMENCLATURE

B	magnetic field, Tesla
C_p	specific heat, J kg^{-1} K^{-1}
g	gravitational acceleration, m s^{-2}
H	cylinder height, m
Ha	Hartmann number $\left(B_0 R_0\sqrt{\sigma_{nf}/\rho_{nf}\nu_f}\right)$
k	thermal conductivity, W m^{-1} K^{-1}
Nu_R	local Nusselt number on thebottom hot disk
Nu_m	Average Nusselt number
p	fluid pressure, Pa
P	dimensionless pressure $\left(\bar{p}R_0^2/\rho_{nf}\alpha_f^2\right)$
Pr	Prandtl number $\left(\nu_f/\alpha_f\right)$
r, z	cylindrical coordinates, m
R, Z	dimensionless coordinates $(r/R_0, z/R_0)$
Ra	Rayleigh number $\left(g\beta_f R_0^3(T_h - T_c)/\nu_f\,\alpha_f\right)$
R_0	cylinder radius, m
S_φ	source term in Eq. (15)
T	temperature, K
u, v	radial, axial velocities, m s^{-1}
U, V	dimensionless radial and axial velocities
α	thermal diffusivity, m^2 s^{-1}
β	thermal expansion coefficient, K^{-1}
ϕ	solid volume fraction
φ	non-dimensional parameter in Eq. (15)
Γ_φ	diffusion term in Eq. (15)
μ	dynamic viscosity, kg^{-1}m^{-1}s^{-1}
ν	kinematic viscosity, m^2 s^{-1}
θ	dimensionless temperature *(T-Tc)/(Th-Tc)*
ρ	density, kg m^{-3}
σ	electrical conductivity, μS cm^{-1}
ψ	dimensionless stream function

Subscripts

ccold, hot

h	hot
f	fluid (pure water)
nf	nanofluid
p	nanoparticle
r, z	radial and axial directions

1. INTRODUCTION

Numerous studies were devoted to numerical and experimental modeling of the natural convection heat transfer problem, because of its wide presence in industrial and technological applications, such as nuclear reactor systems, heating and cooling buildings,solar technology, grain storage, food and metallurgical industries. Enhancement of heat transfer in such systems is very fundamental from the energy saving perspectives. Aprincipal constraint against enhancing the heat transfer in such systems is low thermal conductivity of the usually used fluids like air, water and oil. An innovative technique, which insert within the fluid, metallic particles of nanometer size hope to increase the thermal conductivity of the mixture was first introduced by Choi (1995). The term nanofluid was then generally used to characterize this type of mixture. Many investigations have been carried out in rectangular and square enclosures which showed an immense increase in thermal conductivity with addition of small amounts of nanoparticles (Purta *et al*., 2003; Oztop and Abu-Nada, 2008; Abu-Nada, 2009). However, very few numerical models have been proposed to predict the natural convection in vertical cylinder. Haddad *et al*.(2012) review experimental, numerical and theoretical studies for natural convection of nanofluid in different types of enclosures. They find that most of numerical results showed that nanofluids significantly improve the heat transfer capability of conventional heat transfer fluid. Whereas, experimental results showed that the presence of nanoparticles deteriorates heat transfer systematically. In some fields of industries, such as crystal growth of semi-conductors, material manufacturing and the geothermal energy extraction, the natural convection is under the influence of a magnetic field. There exist several studies (Okada and Ozoe, 1989 and 1992; Garandet at al., 1992; Kolsi *et al*. 2007; Kherief *et al*., 2012) dedicated to understanding the influence of magnetic field on the flow behavior and the heat transfer in the enclosures that are filled with electrically conducting fluids. The most significant results occur in this context is the existence of Lorentz force that affects heat transfer rate. The application of magnetic field, decrease the heat transfer rate and the use of nanofluid enhance the heat transfer in the enclosure. In some engineering systems like the magnetic fields sensors, the magnetic storage media and the cooling systems of electronic equipment, the application of magnetic field is necessary and the enhanced heat transfer rate is desirable. The idea of using nanofluids as working fluid in an enclosure to improve the heat transfer performance in such devices was first presented by Ghasemi *et al*. (2011). The authors investigated the effect of transverse magnetic field on the natural convection in a nanofluid filling a square enclosure and they studied the effects of appropriate parameters such as Rayleigh number, Hartmann number and solid volume fraction on the heat transfer performance of the enclosure. They find that the heat transfer rate increases with an increase of Rayleigh number but it decreases with an increase of the Hartmann number. Depending on the value of Hartmann number and Rayleigh number, an increase of the solid volume fraction may result in enhancement or deterioration of the heat transfer performance.

Aminossadati *et al*. (2011) examined numerically the laminar forced convection of a water-Al_2O_3 nanofluid flowing through a horizontal micro-channel. The middle section of the micro-channel is heated by a constant and uniform heat flux and influenced by a transverse uniform magnetic field. The results show that the micro-channel performs better heat transfers at higher values of the Reynolds and Hartmann numbers. For all values of the Reynolds and Hartmann numbers considered in this study, the average Nusselt number on the middle section surface of the micro-channel increases as the solid volume fraction increases. The rate of this increase is considerably more at higher values of the Reynolds number and at lower values of the Hartmann number. Abouali *et al*. (2012); made a critical review on the subject of numerical simulation of natural convection in enclosures filled with nanofluids. It was shown that based on the assumption of single phase flow idea for the nanofluids, the same correlations exist for prediction of pure fluids heat transfer rate could also be used to predict the overall heat performance of enclosures filled with nanofluids. It was also found that the results of numerical simulations and those existing correlations would coincide if the correlation proposed by Corcione (2011) is used for calculation of the effective thermal conductivity and viscosity. Syam *et al*. (2012) evaluated experimentally the convection heat transfer coefficient and friction factor characteristics of Fe_3O_4 nanofluid for flow in a circular tube. They found that nanofluid heat transfer is higher compared to water and increases with volume concentration. Mahmoudi *et al*. (2013) investigated numerically the entropy generation and enhancement of heat transfer in natural convection flow and heat transfer using copper Cu-water nanofluid in the presence of a constant magnetic field. The analysis uses a two-dimensional trapezoidal enclosure with the left vertical wall and inclined walls kept in a low constant temperature and a heat source with constant heat flux placed on the bottom wall of the enclosure. Their results show that at $Ra=10^4$ and 10^5 the enhancement of the Nusselt number due to the presence of nanoparticles increases with the Hartmann number, but at higher Rayleigh number, a reduction has been observed. Reza Ashorynejad *et al*. (2013) investigated numerically the effect of static radial magnetic field on natural convection heat transfer in a horizontal cylindrical annulus enclosure filled with nanofluid. The inner and the outer cylinder surfaces are maintained at the different uniform temperatures. The results reveal that the flow oscillations can be suppressed effectively by imposing an external radial magnetic field. Also, it is found that the average Nusselt number is an increasing function of nanoparticle volume fraction and Rayleigh number, while it is a decreasing function of Hartmann number.Nasrin and Alim (2014) examined

numerically the influence of nanofluid with double nanoparticles on the forced convection in a flat plate solar collector, they compared heat transfer phenomena among four nanofluids. They found that the average Nusselt number for water-Ag nanofluid is higher than others.

To the best of our knowledge, no attempts have been made as yet to study the effect of the direction of an external applied magnetic field on nanofluid natural convection in a vertical cylinder. The main objective of the present research is an investigation of the effect of various parameters such as Rayleigh number, Hartmann number and solid particle volume fraction on the steady natural convection in a vertical cylinder filled with an Al_2O_3 nanofluid under two different external magnetic fields either in the radial (B_r) or axial (B_z) directions.

2. PROBLEM FORMULATION

Figure 1 shows a schematic diagram of the vertical cylindrical enclosure having an aspect ratio $H/R_0=1$ and filled with water-Al_2O_3 nanofluid. The bottom disk is maintained at a hot temperature T_h, while the top disk is maintained at a cold temperature T_c ($T_c<T_h$). The sidewall of the cylinder is assumed to be adiabatic.It is assumed that the Al_2O_3 nanoparticles and water are in thermal equilibrium and the nanofluid is Newtonian and incompressible.

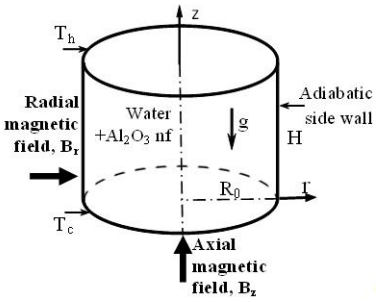

Fig. 1. Geometry of the problem.

Two different external magnetic fields either in the radial (B_r) or axial (B_z) directions are applied. The thermo-physical properties of the base fluid and the nanoparticles presented in Table 1aregiven by Abu-Nada *et al*. (2008). The Boussinesq approximation for buoyancy flow is adopted.Therefore, the governing equations are written in dimensional form as follows:

Table 1 Thermo-physical properties of water and nanoparticles

	Pure Water	Alumina (Al_2O_3)
Pr	6.2	
ρ (kg/m^3)	997.1	3970
C_p (J/kg K)	4179	765
k (W/m K)	0.613	40
β (K^{-1})	21×10^{-5}	0.85×10^{-5}

Continuity equation in both directions of magnetic field:

$$\frac{\partial(ru)}{\partial r}+\frac{\partial(rv)}{\partial z}=0 \qquad (1)$$

The magnetic field is radial:

r-Momentum equation:

$$u\frac{\partial u}{\partial r}+v\frac{\partial u}{\partial z}=\frac{1}{\rho_{nf}}\left[-\frac{\partial P}{\partial r}+\mu_{nf}\left(\frac{1}{r}\frac{\partial}{\partial r}\left(r\frac{\partial u}{\partial r}\right)+\frac{\partial^2 u}{\partial z^2}-\sigma_{nf}B_0^2u\right)\right] \qquad (2)$$

z-Momentum equation:

$$u\frac{\partial v}{\partial r}+v\frac{\partial v}{\partial z}=\frac{1}{\rho_{nf}}\left[-\frac{\partial P}{\partial z}+\mu_{nf}\left(\frac{1}{r}\frac{\partial}{\partial r}\left(r\frac{\partial v}{\partial r}\right)+\frac{\partial^2 v}{\partial z^2}+(\rho\beta)_{nf}g(T-T_c)\right)\right] \qquad (3)$$

The magnetic field is axial:

r-Momentum equation:

$$u\frac{\partial u}{\partial r}+v\frac{\partial u}{\partial z}=\frac{1}{\rho_{nf}}\left[-\frac{\partial P}{\partial r}+\mu_{nf}\left(\frac{1}{r}\frac{\partial}{\partial r}\left(r\frac{\partial u}{\partial r}\right)+\frac{\partial^2 u}{\partial z^2}\right)\right] \qquad (4)$$

z-Momentum equation:

$$u\frac{\partial v}{\partial r}+v\frac{\partial v}{\partial z}=\frac{1}{\rho_{nf}}\left[-\frac{\partial P}{\partial z}+\mu_{nf}\left(\frac{1}{r}\frac{\partial}{\partial r}\left(r\frac{\partial v}{\partial r}\right)+\frac{\partial^2 v}{\partial z^2}+(\rho\beta)_{nf}g(T-T_c)-\sigma_{nf}B_0^2v\right)\right] \qquad (5)$$

Energy equation in both directions of magnetic field:

$$u\frac{\partial T}{\partial r}+v\frac{\partial T}{\partial z}=\alpha_{nf}\left[\frac{1}{r}\frac{\partial}{\partial r}\left(r\frac{\partial T}{\partial r}\right)+\frac{\partial^2 T}{\partial z^2}\right] \qquad (6)$$

In the above equations, the density of nanofluid is assumed to be constant, except in the buoyancy term $\left(-(\partial p/\partial z)-\rho_{nf}g\right)$ in the z-momentum equation. The buoyancy term can be written as$-(\partial\bar{p}/\partial z)+\left(\rho_c-\rho_{nf}\right)g$, where $\bar{p}$ is the modified pressure ($\bar{p}=p+\rho_c gz$) and ρ_c is the density of nanofluid at the reference temperature, T_c.

By using the definition of nanofluid thermal expansion coefficient,$\beta_{nf}=-\left(1/\rho_{nf}\right)(\partial\rho/\partial T)_p$, the buoyancy term in the z direction can be rewritten as: $-(\partial\bar{p}/\partial z)+(\rho\beta)_{nf}g(T-T_c)$.
The classical models reported in the literature by Brinkman (1952) are used to determine the properties of the nanofluid.

The thermal diffusivity in equation (6) is given as:

$$\alpha_{nf}=k_{nf}/\left(\rho C_p\right)_{nf} \qquad (7)$$

The electrical conductivity of the nanofluid is given as:

$$\sigma_{nf}=(1-\emptyset)\sigma_f+\emptyset\sigma_p \qquad (8)$$

The effective density of the nanofluid is expressed as:

$$\rho_{nf}=(1-\emptyset)\rho_f+\emptyset\rho_p \qquad (9)$$

The heat capacitance of the nanofluid is expressed

Table 2 A summary of non-dimensional governing equations

Eqs	φ	Γ_φ	S_φ (B_r)	S_φ (B_z)
Conti-nuity	1	0	0	0
R-mom-entum	U	$\frac{\mu_{nf}}{\rho_{nf}\alpha_f}$	$-\frac{\partial P}{\partial R} - Ha^2 PrU$	$-\frac{\partial P}{\partial R}$
Z-mom-entum	V	$\frac{\mu_{nf}}{\rho_{nf}\alpha_f}$	$-\frac{\partial P}{\partial Z} + \frac{(\rho\beta)_{nf}}{\rho_{nf}\beta_f} RaPr\theta$	$-\frac{\partial P}{\partial Z} + \frac{(\rho\beta)_{nf}}{\rho_{nf}\beta_f} RaPr - Ha^2 PrV$
Ene-rgy	T	$\frac{\alpha_{nf}}{\alpha_f}$	0	0

as:

$$\left(\rho C_p\right)_{nf} = (1-\emptyset)\left(\rho C_p\right)_f + \emptyset\left(\rho C_p\right)_p \quad (10)$$

The thermal expansion of the nanofluid is given as:

$$(\rho\beta)_{nf} = (1-\emptyset)(\rho\beta)_f + \emptyset(\rho\beta)_p \quad (11)$$

The effective dynamic viscosity and thermal conductivity of the nanofluid are modeled by Brinkman (1952)and Maxwell (1873)

$$\mu_{nf} = \mu_f(1-\emptyset)^{-2.5} \quad (12)$$

$$k_{nf} = k_f\left[\frac{(k_p+2k_f)-2\emptyset(k_f-k_p)}{(k_p+2k_f)+\emptyset(k_f-k_p)}\right] \quad (13)$$

By introducing the dimensionless parameters defined as follows:

$$R=\frac{r}{R_0},\quad Z=\frac{z}{R_0},\ U=\frac{u}{(\alpha_f/R_0)},\ V=\frac{v}{(\alpha_f/R_0)},$$

$$P=\frac{\bar{p}\,R_0^2}{\rho_{nf}\alpha_f^2},\ \theta=\frac{T-T_c}{T_h-T_c}, Ra=\frac{g\beta_f R_0^3(T_h-T_c)}{\nu_f\alpha_f},$$

$$Ha=B_0R_0\sqrt{\frac{\sigma_{nf}}{\rho_{nf}\nu_f}}, Pr=\frac{\nu_f}{\alpha_f} \quad (14)$$

The dimensionless form of the governing equations (1)-(6) are presented as:

$$\frac{\partial(U\varphi)}{\partial R}+\frac{\partial(V\varphi)}{\partial Z}=\frac{\partial}{\partial R}\left(\Gamma_\varphi\frac{\partial\varphi}{\partial R}\right) + \frac{\partial}{\partial Z}\left(\Gamma_\varphi\frac{\partial\varphi}{\partial Z}\right)+S_\varphi \quad (15)$$

Where φ stands for the dependent dimensionless parameters U, V and θ and Γ_φ and S_φ are the corresponding diffusion and source terms, respectively, as summarized in Table 2.

The governing equations are subject to the following boundary conditions:

Symmetry axe:

$$\text{At}\quad R=0\quad U=\frac{\partial V}{\partial R}=0\ \frac{\partial\theta}{\partial R}=0 \quad (16a)$$

Adiabatic lateral wall:

$$\text{At}\quad R=1 U=V=0 \qquad \frac{\partial\theta}{\partial R}=0 \quad (16b)$$

Hot bottom disk:

$$\text{At}\quad Z=0\quad U=V=0 \qquad \theta=1 \quad (16c)$$

Cold top disk:

$$\text{At} Z=\frac{H}{R_0}\quad U=V=0 \quad \theta=0 \quad (16d)$$

The local Nusselt number on the top cold disk is defined by:

$$Nu_R(R) = -\frac{k_{nf}}{k_f}\left(\frac{\partial\theta}{\partial Z}\right)_{Z=H/R_0} \quad (17)$$

The average Nusselt number (Nu_m) is determined by integrating the local Nusselt along the hot disk:

$$Nu_m = \int_0^1 Nu_R(R)dR \quad (18)$$

3. NUMERICAL APPROACH AND VALIDATION

The non-dimensional governing equations (15) with the associated boundary conditions (16) were discretized using a finite-volume formulation given by Patankar (1980). The vectorial quantities (u and v) are stored on the faces of volumes and the scalar quantities (P and θ) are stored in the centers. For the convection and diffusion fluxes were approximated by a second-order accurate central differencing schemeand the SIMPLER algorithm was utilized to handle the pressure-velocity coupling. Finally, the discretized algebraic equations are solved by the line-by-line tri-diagonal matrix algorithm (TDMA). The numerical method was implemented in a FORTRAN program.

3.1 Grid Independency Study

The effect of grid resolution was examined for ϕ =0.1, Ra= 10^4, and Ha=10 (B_r), in order to select the appropriate grid density. Results given in Fig. 2 show that a grid size of 112×112 nodes satisfies the grid independence. This grid is therefore adopted for all numerical simulations, in order to optimize theCPU time and the cost of computations.

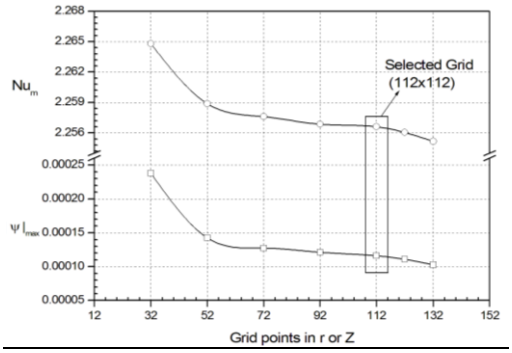

Fig. 2. Result of grid independence at ϕ=0.1, Ra=10^4, Ha=10 (B_r).

3.2 Validation of the Computer Code

The results of our numerical simulations have been

compared to the numerical results of Ghasemi *et al*. (2011). Figure 3. Shows the dimensionless y-velocity along the horizontal mid-span of the enclosure for Rayleigh number $Ra=10^5$, solid volume fraction ϕ =0.03 and Hartmann numbers Ha=0, 30 and 60. Figure 4 provides also, the comparisons of streamlines (a) and(c), and isotherms (b) and (d) with the same workfor Rayleigh number $Ra=10^5$, solid volume fraction ϕ =0.03 and Hartmann number Ha=30.It can be seen, that a good agreement is obtained

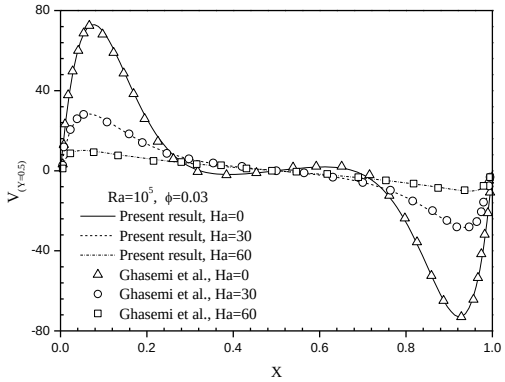

Fig. 3. Validation of the present code with results of Ghasemi *et al*. (2011).

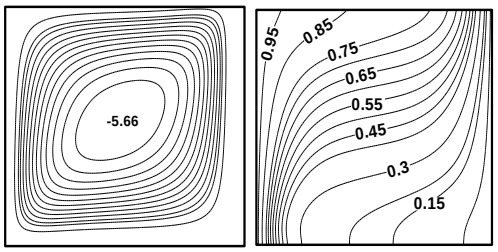

(a) (b)

Present results

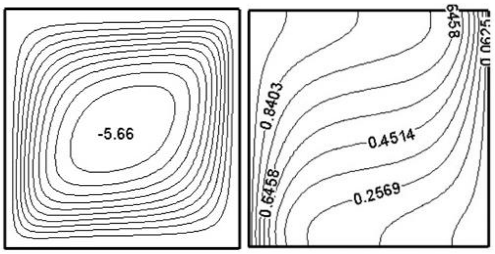

(c) (d)

Results of Ghasemi *et al*. (2011)

Fig. 4. Validation of the present code with results of Ghasemi *et al*. (2011) for $Ra=10^5$, ϕ=0.03 and Ha=30: Streamlines(a) and (c), Isotherms (b) and (d).

4. RESULTS AND DISCUSSION

The cylinder is filled with a water-Al_2O_3 nanofluid. Streamlines and isotherms for $Ra=10^4$ with three values of the solid volume fraction (ϕ=0, 0.04, 0.1) without magnetic field (Ha=0) and with two values of Hartmann number (Ha=10 and Ha=80) for either in the radial or axial directions of magnetic field are presented in fig.5 and fig. 6. All variables U, V, θare given in dimensionless form. In fig.5 which illustrates the streamlines, the buoyancy-driven circulating flows within the cylinder are evident for all values of Hartmann numbers and for both directions of the magnetic field. By adding the magnetic field intensity, the strength of circulation decreases and this decrease is more pronounced if the magnetic field direction is orientedaxially (B_z). That is to say, the addition of nanoparticles to pure water (ϕ =0) reduces the strength of the flow field, as observed by other researchers such as Ho *et al*. (2008). If the magnetic field is oriented radially (B_r), the vortex core stretches vertically. The shape of the vortex changes from circular to elliptic. This phenomenon is due to the magnetic force, which is against the flow direction and causes a considerable reduction in the intensity of streamlines. In addition, by increasing the solid volume fraction, the intensity of circulation decreases but the trends of the vortex do not change.Figure6 shows that by applying the magnetic field, the flow field is affected and subsequently, the dominant mechanism of heat transfer changes. The magnetic field has a negative effect on buoyancy force and decrease the flow motion. This reduction in velocity causes a decrease in the convection heat transfer.At Ha=10, it is clear that the isotherms are affected by variation in the solid volume fraction and by the magnetic field direction.

The domination of the conduction regime which appear in horizontal isotherms is more important if the magnetic field is oriented axially and with the increasing of solid volume fraction (Ha=10, ϕ=0.1). The results also show a conduction-dominated regime with horizontal isotherms at high Hartmann numbers (Ha=80). Figure7 presents the dimensionless axial velocity profiles along the midsection (middle plane) of the cylindrical enclosure. It can be seen from this figure the effects of the solid volume fraction on the axial velocity and the effect of the application of the magnetic field (Ha=40 and Ha=80) in either directions axial and radial for two values of Rayleigh number $Ra=10^3$ and 10^4. It is clear that as the solid volume fraction of the Al_2O_3 nanoparticles increases the absolute magnitude of vertical velocity decreases. This decrease is due to the suppression of buoyant flows of the nanofluid at a higher solid volume fraction of the nanoparticles in the nanofluid. In addition, the increase in Hartmann number dramatically decreases the amount of vertical velocity. The absolute magnitude of velocity increases with Rayleigh number, because increasing this number means increasing buoyancy force.In fig.8, it is observed that the Hartmann number has an insignificant influence on the temperature profiles, because the heat transfer of

these important values of Hartmann numbers (Ha=40, Ha=80) at these two values of the Rayleigh

number ($Ra=10^3$ and $Ra=10^4$) is mainly due to the conduction. In addition, this figure shows that the

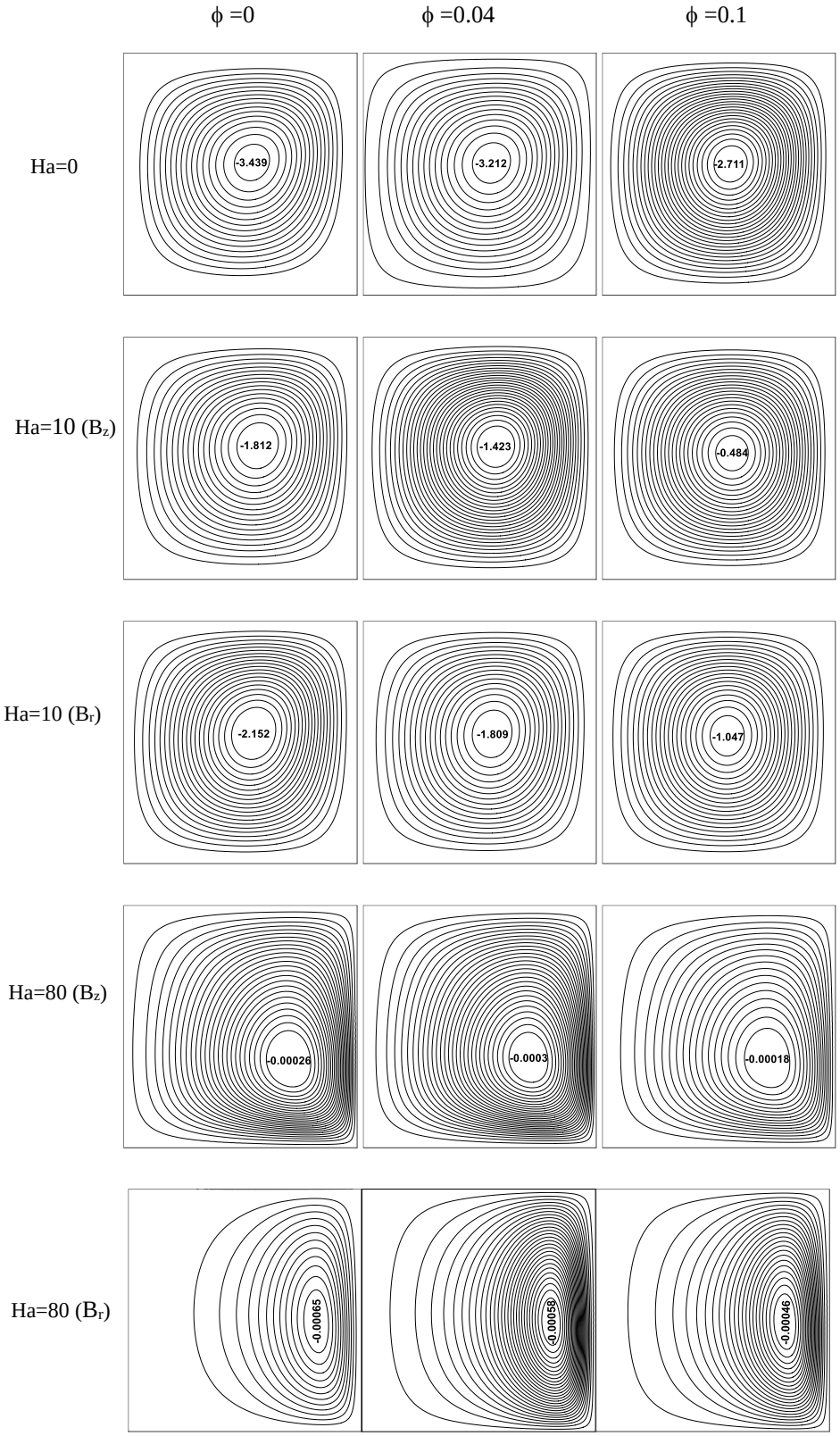

Fig.5. Streamlines at Ra=10^4 for different Hartmann numbers Ha (radial B_r and axial B_z magnetic fields) and solid volume fractions ϕ.

increasing of the solid volume fraction of nanoparticles in nanofluid increases the temperature at the mean part of the cylindrical enclosure and decreases it near the adiabatic sidewall.

Figures 9a-b illustrate the variation of dimensionless radial velocity U along the height ofthe cylinder at Ha=10 (axial B_z and radial B_r magnetic fields) and for two values of ϕ. It shows

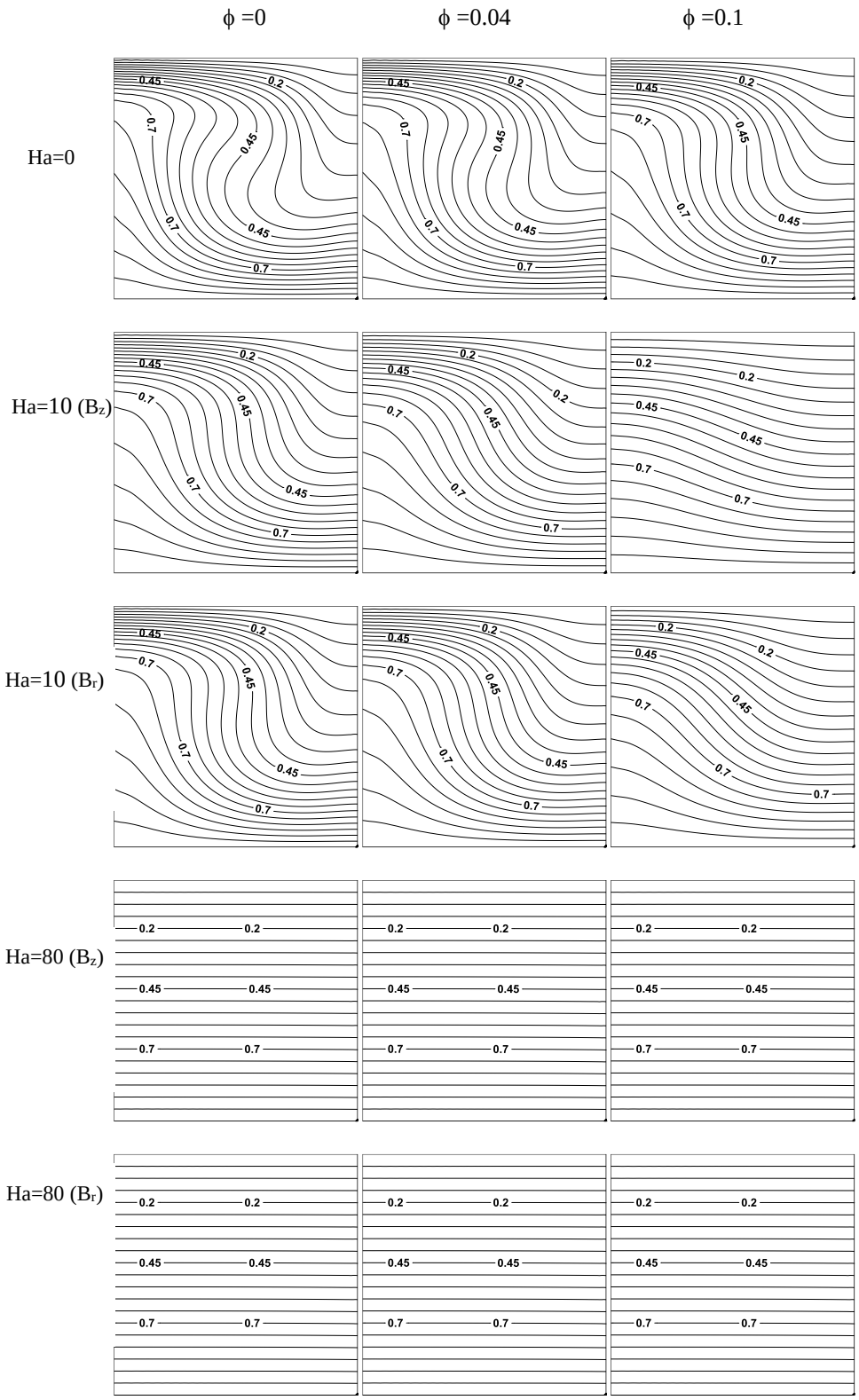

Fig.6. Isotherms at Ra=10^4 for different Hartmann numbers Ha (radial B_r and axial B_z magnetic fields) and solid volume fractions ϕ.

that the enhancement in the buoyancy-force due to the increase of Rayleigh number increment substantially the radial velocity, and the enhancement of the solid volume fraction reduce the radial velocity and this reduction is more considerable if the magnetic field direction is axial and this has a good corresponding with results found previously.Figure 10 shows the effect of Hartmann number Ha (radial B_r and axial B_z magnetic fields) on the variation of the average

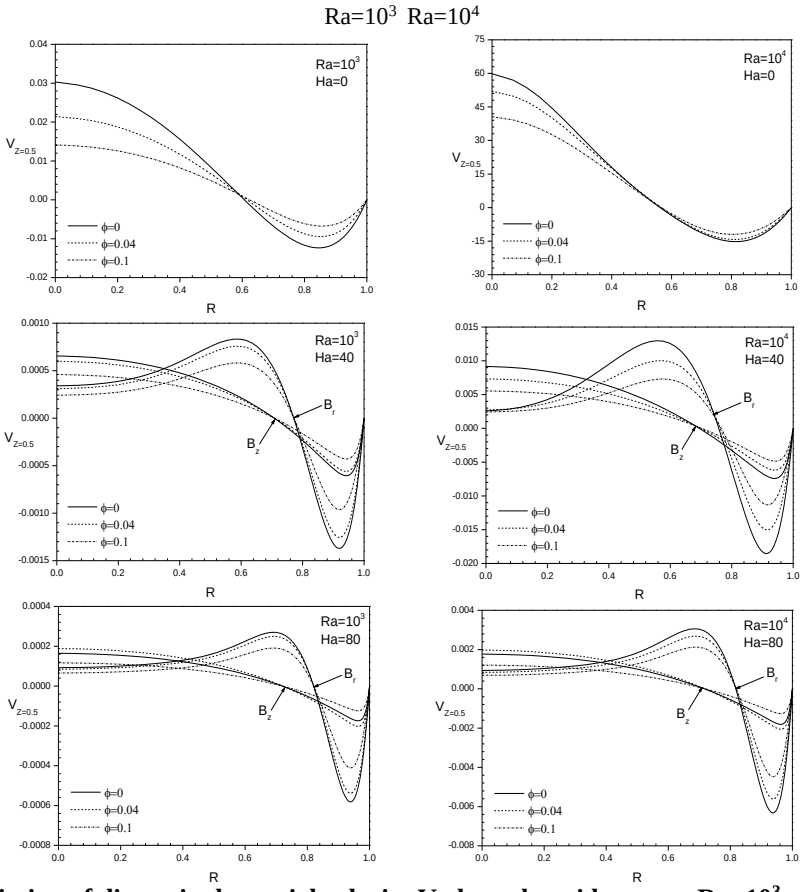

Fig. 7. Variation of dimensionless axial velocity V along the mid-span at Ra=10^3 and Ra=10^4 and different values of ϕ.

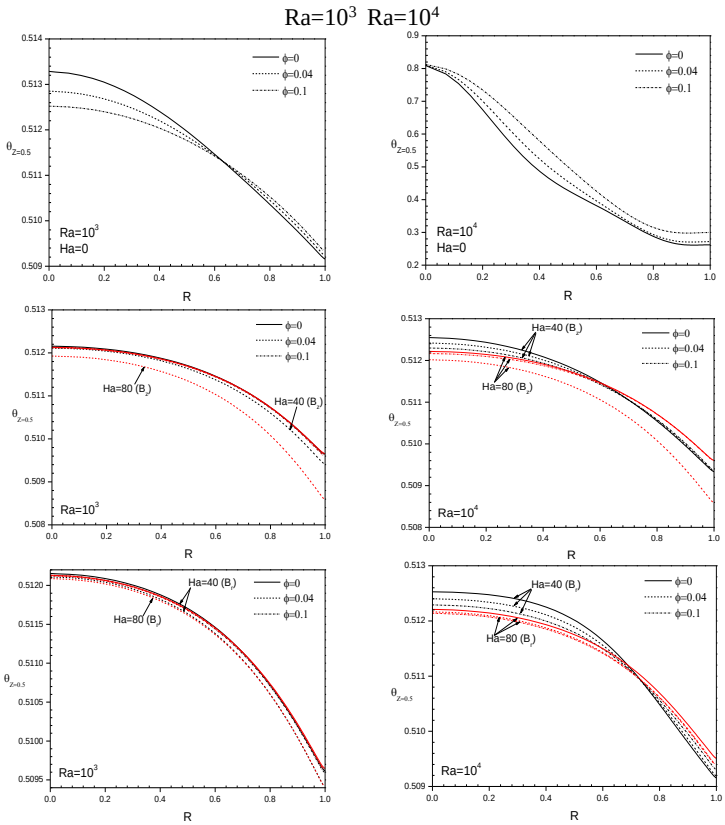

Fig. 8. Variation of dimensionless temperature θ along the mid-span at Ra=10^3 (left) and Ra=10^4 (right) and for different values of ϕ.

Nusselt number Nu_m at ϕ=0.04 and for two values of Rayleigh number when the cylindrical enclosure is filled with a water-Al_2O_3 nanofluid (ϕ=0.04). For $Ra=10^3$, where the heat transfer is only due to conduction and the magnetic field does not have an important effect on the heat transfer performance, the average Nusselt number remains unchanged when the Hartmann number increases. The average Nusselt number does, however, decrease for $Ra=10^4$ if Ha<20 when the heat transfer is mainly due to convection and this decrease is more important if the magnetic field is applied in axial direction (B_z). For Ha≥20, the magnetic field suppresses the convection flows, so that the average Nusselt number becomes practically constant.

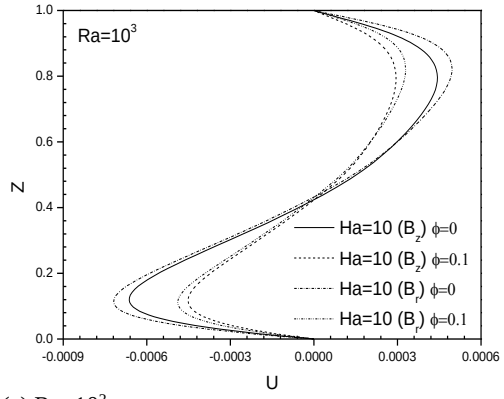

(a) $Ra=10^3$

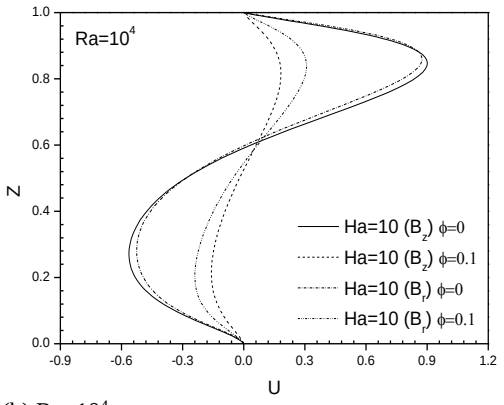

(b) $Ra=10^4$

Fig. 9. Variation of dimensionless radial velocity U along the height of the cylinder at Ha=10 (axial B_z and radial B_r magnetic fields) and for two values of ϕ.

For $Ra=10^4$, table 3 illustrates the variation of the average Nusselt number (Nu_m) and the maximum stream function ($|\Psi|_{max}$) with the solid volume fraction at different values of the Hartmann number either in the radialor axial directions of the magnetic field. The values show that the solid volume fraction has an important influence on the heat transfer performance of the cylindrical enclosure at all values of the Hartmann numbers.For Ha≤20, it is clear that the Nusselt number decreases strongly with the increasing Hartmann number, especially when the magnetic field is applied in axial direction.

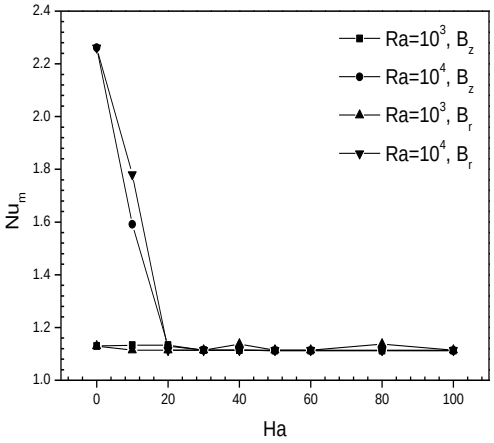

Fig. 10. The effect of Hartmann number (radial B_r and axial B_z magnetic fields) on the variation of the average Nusselt number at ϕ=0.04 and for two values of Rayleigh number.

Table 3 Average Nusselt number and the maximum steam function at various Ha and ϕ ($Ra=10^4$)

Ha	ϕ=0 Nu_m	ϕ=0.04N u_m	ϕ=0.1 Nu_m
0	2.2053	2.2616	2.2566
10 B_z	1.6634	1.5754	1.3762
B_r	1.8445	1.7806	1.5840
20 B_z	0.9956	1.1140	1.3090
B_r	1.0430	1.1141	1.3108
40 B_z	0.9952	1.1138	1.3106
B_r	0.9953	1.1139	1.3106
80 B_z	0.9954	1.1125	1.3107
B_r	0.9953	1.1138	1.3105
	$\|\Psi\|_{max}$	$\|\Psi\|_{max}$	$\|\Psi\|_{max}$
0	3.9934	3.8020	3.3994
10 B_z	2.3935	2.1420	1.7175
B_r	2.6923	1.8062	1.0469
20 B_z	0.9486	0.7607	0.5515
B_r	1.3440	1.0912	0.7761
40 B_z	0.2363	0.1981	0.1565
B_r	0.3878	0.3201	0.2486
80 B_z	0.0638	0.0547	0.0443
B_r	0.1173	0.1003	0.0807

As the Nusselt number describes the intensity of the convective heat transfer this observation indicates clearly the significant inhibition of the convective heat transfer by the magnetic field at Ha>20. For all values of Hartmann number, if the solid volume fraction increases $|\Psi|_{max}$ is reduced. The addition of solid nanoparticles to the base fluid involves an increase of μ_{nf}/ρ_{nf} in the diffusive term. This means weaker circulation flow and lower values of the maximum stream function. Also, for Ha=10, as thesolid volume fraction increases the heat transfer rate decreases. For high values of the Hartmann number (Ha≥20), an increase of the solid volume fraction results in the increase of the heat transfer performance.

Figure 11 illustrates the effect of Hartmann number Ha (axial magnetic field, B_z) on the variation of the average Nusselt number Nu_m at $Ra=10^4$ and for different values of ϕ.We can observe the increase in the heat transfer performance in the case of an axial direction of the magnetic field with the increasing in solid volume fraction ϕ.

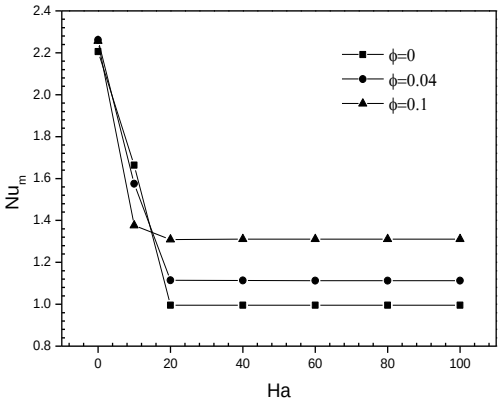

Fig. 11. The effect of Hartmann number Ha (axial magnetic field, B_z) on the variation of the average Nusselt number Nu_m at $Ra=10^4$ and for different values of ϕ.

Figure 12 shows the variation of local Nusselt number Nu_R along the top cold disk at $Ra=10^4$ and Ha=10 (radial B_r and axial B_z magnetic fields) for different values of ϕ. The results show that if the solid volume fraction increases the local Nusselt number decreases in both directions of the magnetic field.Also, it is shown that the local Nusselt number when the magnetic field is applied axially is less than the one when the magnetic field is applied radially and this result is in good agreement with earlier finding.The effect of solid volume fractionϕ on the variation of the average Nusselt number ratio ($Nu_m/Nu_{m,\phi=0}$) at $Ra=10^4$ and for different Hartmann numbers (radial B_r and axial B_z magnetic fields) is presented in fig. 13.The results presented for Rayleigh number $Ra=10^4$ show that as the Hartmann number increases fromHa=0 to Ha=10, the average Nusselt number ratio decreases when the solid volume fraction increases and the rate of this decrease is more important if the magnetic field direction is axial. For Ha ≥ 20, the average Nusselt number ratio increases as the solid volume fraction increases. This behavior is due to the great effect of the magnetic field and its stronger suppression of the buoyant flows in the nanofluid.

Table 4 presents the effect of the solid volume fraction (ϕ) on the average Nusselt number (Nu_m) and the maximum stream function ($|\Psi|_{max}$) at two values of the Rayleigh number ($Ra=10^3$ and $Ra=10^4$).

The value of Hartmann number considered is Ha=20. For these two values of the Rayleigh number, the buoyant forces are weak and diffusion governs the behavior of the fluid. The addition of nanoparticles results in weaker buoyancy-driven circulations and low values of maximum stream function. That being said, the heat transfer rate still expected to increase as the solid volume fraction increases. This finding is similar to that of the previous results.

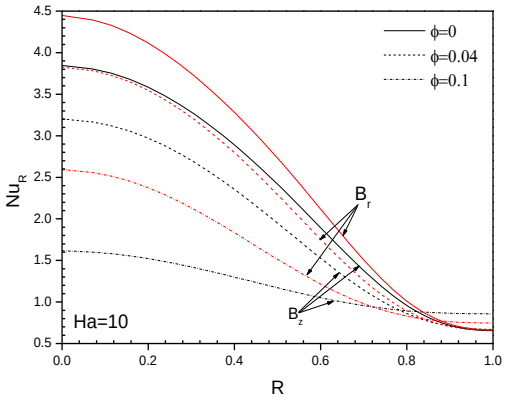

Fig. 12. Variation of local Nusselt number Nu_R along the top cold disk at $Ra=10^4$ and Ha=10 (radial B_r and axial B_z magnetic fields) for different values of ϕ.

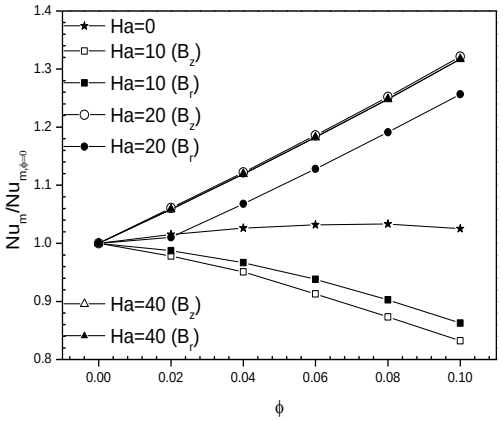

Fig. 13. The effect of solid volume fraction ϕ on the variation of the average Nu number ratio at $Ra=10^4$ and for different Hartmann numbers.

Table 4 Average Nusselt number and the maximum steam function at various ϕ and at $Ra=10^3$ and $Ra=10^4$ (Ha=20)

ϕ		Ha=20 (B_z)		Ha=20 (B_r)	
		$Ra=10^3$	$Ra=10^4$	$Ra=10^3$	$Ra=10^4$
0	Nu_m	0.9954	0.9956	0.9953	1.0432
	$\|\Psi\|_{max}$	0.0632	0.9486	0.8394	1.3440
0.02	Nu_m	1.0523	1.0524	1.0533	1.0540
	$\|\Psi\|_{max}$	0.0584	0.8506	0.0776	1.2160
0.06	Nu_m	1.1757	1.1756	1.1756	1.1769
	$\|\Psi\|_{max}$	0.0503	0.6808	0.0666	0.9746
0.1	Nu_m	1.3087	1.3090	1.3107	1.3108
	$\|\Psi\|_{max}$	0.0436	0.5515	0.0576	0.7761

5. CONCLUSION

Natural convection in a cylindrical enclosure filled with a water-Al_2O_3 nanofluid and under two different external magnetic fields (B_r, B_z) either in the radial or axial directions has been studied numerically. The effect of the magnetic field

direction and some parameters such as the solid volume fraction and the Hartmann number on the flow and temperature fields, and heat transfer rate have been examined.

The main conclusions are summarized as follows:

The magnetic field reduces the circulation in the cylindrical cavity, when the magnetic field becomes stronger.

If the conduction regime dominates, the strength and direction of the magnetic field have a weakness influence on the heat transfer rate, but the increasing of solid volume fraction increment considerably the heat transfer performance for all values of Hartmann number.

For low values of Hartmann numbers (Ha<20) and at Rayleigh number $Ra=10^4$ where the convection mode remains dominate, the increasing in solid volume fraction in the nanofluid decreases the heat transfer performance, especially if the magnetic field is applied axially.

ACKNOWLEDGEMENTS

The authors gratefully acknowledge the financial support of this work through the project n° J0300920110029 provided by the Algerian Ministry of High Education and Scientific Research.

REFERENCES

Abouali, O. and G. Ahmadi (2012). Computer Simulations of Natural Convection of Single Phase Nanofluids in Simple Enclosures: A critical Review. *Applied Thermal Engineering* 36, 1-13.

Abu-Nada, E. (2009). Effects of Variable Viscosity and Thermal Conductivity of Al_2O_3-Water Nanofluid on Heat Transfer Enhancement in Natural Convection. *Int. J. Heat and Fluid Flow* 30, 679-690.

Abu-Nada, E., Z. Masoud and A. Hijazi (2008). Natural Convection Heat Transfer Enhancement in Horizontal Concentric Annuli Using Nanofluids. *International Communication in Heat and Mass Transfer* 35, 657-665.

Aminossadati, S. M., A. Raisi and B. Ghasemi (2011).Effects of Magnetic Field on Nanofluid Forced Convection in a Partially Heated Microchannel. *Int. J. Non-Linear Mechanics* 46,1373-1382.

Brinkman, H. C. (1952). The Viscosity of Concentrated Suspensions and Solution. *The Journal of Chemical Physics* 571-581.

Choi, S. U. S. (1995). Enhancing Thermal Conductivity of Fluids with Nanoparticles. *ASME Fluids Engineering Division* 231, 99-105.

Corcione, M. (2011). Empirical Correlating Equations for Predicting the Effective Thermal Conductivity and Dynamic Viscosity of Nanofluids. *Energy conversion and Management* 52, 789-793.

Garandet, J. P., T. Alboussière and R. Moreau (1992). Buoyancy Driven Convection in a Rectangular Enclosure with a Transverse Magnetic field. *Int. J. Heat Mass Transfer* 35, 741-748.

Ghasemi, B., S. M. Aminossadati and A. Raisi (2011). Magnetic Field Effect on Natural Convection in a Nanofluid-filled Square Enclosure. *Int. J Thermal Sciences*, 50, 1748-1756.

Haddad, Z., F. Oztop, E. Abu-Nada and A. Mataoui (2012). A Review on Natural Convective Heat Transfer of Nanofluids. *Renewable and Sustainable Energy Reviews* 16, 5363-5378.

Ho, C. J., M. W. Chen and Z. W. Li (2008). Numerical Simulation of Natural Convection of Nanofluid in a Square Enclosure: Effects due to Uncertainties of Viscosity and Thermal Conductivity. *Int. J. Heat Mass Transfer* 51, 4506-4516.

Kherief, M. N., K. Talbi and F. Berrahil (2012). Effects of Inclination and Magnetic Field on Natural Convection Flow Induced by a Vertical Temperature. *Journal of Applied Fluid Mechanics* 5(1), 113-120.

Kolsi, A., A. Abidi, M. N.Borjini, N. Daous and H. Ben Aissia (2007). Effect of an External Magnetic Field on the 3-D Unsteady Natural Convection in a Cubical Enclosure. *Numerical Heat Transfer, PartA* 51, 1003-1021.

Mahmoudi, A., I. Pop, M. Shahi and F. Talbi (2013). MHD Natural Convection and Entropy Generation in a Trapezoidal Enclosure Using Cu-water Nanofluid. *Computers & Fluids* 72, 46-62

Maxwell, J. C. (1873). *A Treatise on Electricity and Magnetism, vol. II*. Oxford University Press, Cambridge, UK 54.

Nasrin, R. and M. A. Alim (2014). Finite Element Simulation of Forced Convection in a Flat Plate Solar Collector: Influence of Nanofluid with Double Nanoparticles. *Journal of Applied Fluid Mechanics* 7(3), 543-556.

Okada, K. and H. Ozoe (1989). The Effect of the Direction of the External Magnetic Field on the Three-Dimensional Natural Convection in a Cubical Enclosure. *Int. J. Heat Mass Transfer* 32, 1939-1954.

Okada, K. and H. Ozoe (1992). Transient Responses of Natural Convection Heat Transfer with Liquid Gallium under an External Magnetic Field in Either the x, y or z Direction.

Industrial & Engineering Chemical Research 31, 700-706.

Oztop, F. and E. Abu-Nada (2008). Numerical Study of Natural Convection in Partially Heated Rectangular Enclosures Filled with Nanofluids. *Int. J. Heat and Fluid Flow* 29, 1326-1336.

Patankar, S. V. (1980). *Numerical Heat Transfer and Fluid Flow*. Hemisphere, Washington, DC.

Putra, N., W. Roetzel and S. K. Das (2003). Natural Convection of Nanofluids. *Heat and Mass Transfer* 39, 775-784.

Syam Sundar, L., M. T. Naik, M. K. Singh and T. Ch. Siva Reddy (2012). Experimental Investigation of Forced Convection Heat Transfer and Friction Factor in a Tube with Fe_3O_4 Magnetic Nanofluid. *International Journal of Experimental Heat Transfer, Thermodynamics and Fluid Mechanics*, ETF science (New York, NK: Elsevier) 37, 65-72.